

Investigation of structural transport and magnetic properties of the system $\text{Li}_{0.25}\text{Cu}_{0.5}\text{Fe}_{2.25-x}\text{Al}_x\text{O}_4$

ASHFAQ AHMAD

Department of Chemistry, The Indian School, PO Box 558, Bahrain

Experimental data on X-ray electrical conductivity, thermoelectric coefficient, magnetic hysteresis and infrared absorption spectra of the system $\text{Li}_{0.25}\text{Cu}_{0.5}\text{Fe}_{2.25-x}\text{Al}_x\text{O}_4$ are presented. All the compounds, $0 \leq x \leq 2.25$, showed cubic symmetry. Lattice constant values progressively decreased on increasing the Al^{3+} content. X-ray intensity calculations, magnetic hysteresis and infrared spectroscopy studies indicated the presence of Li^+ , Al^{3+} and Fe^{3+} at tetrahedral and octahedral sites, while Cu^{2+} is present only at the octahedral site. The activation energy and threshold frequency increased with increasing values of x . The compounds with $x \leq 1.50$ are *n*-type, and those with $x \geq 2.0$ are *p*-type semiconductors. Magnetic hysteresis indicated that compounds with $x \leq 1.50$ are ferrimagnetic, and those with $x \geq 2.0$ are antiferromagnetic. High coercive force, H_c , values and remanence ratios (J_R/J_S) showed that all the compounds except $x \geq 2.0$ exhibit single-domain behaviour. The probable ionic configuration for the system is suggested as $\text{Li}_{0.15}^+\text{Al}_{0.5}^{3+}\text{Fe}_{0.35}^{3+}[\text{Li}_{0.1}^+\text{Cu}_{0.5}^{2+}\text{Fe}_{0.4}^{3+}\text{Al}^{3+}]\text{O}_4^{2-}$.

1. Introduction

The transition-metal oxides with a spinel structure have attracted widespread attention because of their remarkable electrical and magnetic properties [1, 2]. These properties are controlled by the oxidation state and distribution of the cations at the tetrahedral and octahedral sites in the lattice. The cation distribution depends on temperature, stoichiometric composition and the method of preparation of the compounds.

The system $\text{Li}_{0.5}\text{Fe}_{2.5-x}\text{Al}_x\text{O}_4$ was studied by Raj and Kulshreshtha [3] using Mossbauer spectroscopy. They found that, due to magnetic dilution carried out by non-magnetic Al^{3+} ions, compounds showed short-range magnetic order and magnetic clusters.

Kapitanova [4] has investigated the cation distribution in lithium galloferrites with varying compositions and firing temperatures. He observed that, for the same composition, the fraction of gallium in the tetrahedral site increases with an increase in firing temperature for the same period of time.

Compounds of the system $\text{Li}_{0.25}\text{Cu}_{0.5}\text{Fe}_{2.25-x}\text{Al}_x\text{O}_4$ were prepared by the standard ceramic techniques and were studied by X-ray, electrical conductivity, thermoelectric power, magnetic hysteresis and infrared spectroscopy to arrive at the probable ionic configuration.

2. Materials and methods

The compositions of the system $\text{Li}_{0.25}\text{Cu}_{0.5}\text{Fe}_{2.25-x}\text{Al}_x\text{O}_4$ (where $0 \leq x \leq 2.25$) were prepared by

the ceramic technique: stoichiometric proportions of Li_2CO_3 , CuO , Fe_2O_3 and $\text{Al}(\text{OH})_3$ (GR grade) powder were ground in acetone. The homogeneous mass was pelletized using a 2% solution of polyvinyl acetate as a binder. The pellets were heated at 700 K in air for the removal of binder, and subsequently sintered at 1173 K for 60 h. X-ray diffractometer (XRD) patterns were recorded on a Philips diffractometer using Cu-K_α radiation with a Ni filter. Conductivity measurements from room temperature to 773 K were carried out by two proven techniques. Thermoelectric coefficients were calculated by taking measurements from 300 to 573 K.

The magnetic hysteresis study was carried out on an alternating-current electromagnet-type hysteresis loop tracer at 80 and 300 K, at an applied field of 3000 Oe. The infrared spectra were recorded at room temperature on an infrared spectrophotometer (Perkin-Elmer 683) from 4000–200 cm^{-1} .

3. Results and discussion

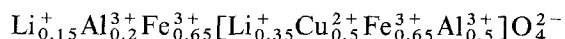
3.1. Structural determination

XRD patterns of all the compositions indicated complete spinel formation, as no lines of individual oxides were seen. All the compounds of the system in the range $0 \leq x \leq 2.25$ crystallized out with cubic structure. The lattice parameter values are shown in Table I, which shows that the lattice constant value, a , progressively decreases on going from

$\text{Li}_{0.25}\text{Cu}_{0.5}\text{Fe}_{2.25}\text{O}_4$ to $\text{Li}_{0.25}\text{Cu}_{0.5}\text{Al}_{2.25}\text{O}_4$. In order to determine the cation distribution, XRD intensities were calculated using the formula

$$|I_{hkl}| = |F_{hkl}|^2 PL_p \quad (1)$$

where F is the structure factor, P is the multiplicity factor and L_p is the Lorentz polarization. The ionic configuration based on site-preference energy values suggested by Miller [5] for individual cations can be written as



The results of intensity calculations for various possible models of $\text{Li}_{0.25}\text{Cu}_{0.5}\text{Fe}_{0.75}\text{Al}_{1.5}\text{O}_4$ are listed in Table II; in Table III, the results for $\text{Li}_{0.25}\text{Cu}_{0.50}\text{Fe}_{2.25}\text{O}_4$ and $\text{Li}_{0.25}\text{Cu}_{0.50}\text{Al}_{2.25}\text{O}_4$ are shown. From these tables, it is observed that copper ions occupy the octahedral site and lithium, aluminium and iron ions occupy both A and B sites. It is

TABLE I Lattice constant activation energy and thermo-electric coefficient values for the system $\text{Li}_{0.25}\text{Cu}_{0.5}\text{Fe}_{2.25-x}\text{Al}_x\text{O}_4$

Compound	Lattice constants a (nm)	Activation energy ΔE (eV)	Thermo electric coefficient α ($\mu\text{V K}^{-1}$)
$\text{Li}_{0.25}\text{Cu}_{0.5}\text{Fe}_{2.25}\text{O}_4$	0.8365	0.397	- 100
$\text{Li}_{0.25}\text{Cu}_{0.5}\text{Fe}_{1.75}\text{Al}_{0.5}\text{O}_4$	0.8298	0.456	- 150
$\text{Li}_{0.25}\text{Cu}_{0.5}\text{Fe}_{1.25}\text{Al}_{1.0}\text{O}_4$	0.8222	0.496	- 350
$\text{Li}_{0.25}\text{Cu}_{0.5}\text{Fe}_{0.75}\text{Al}_{1.5}\text{O}_4$	0.8220	0.515	- 212.5
$\text{Li}_{0.25}\text{Cu}_{0.5}\text{Fe}_{0.25}\text{Al}_{2.0}\text{O}_4$	0.8160	0.536	+ 342
$\text{Li}_{0.25}\text{Cu}_{0.5}\text{Al}_{2.25}\text{O}_4$	0.8150	0.675	+ 250

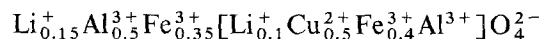
TABLE II Comparison of intensity ratios for $\text{Li}_{0.25}\text{Cu}_{0.5}\text{Fe}_{0.75}\text{Al}_{1.5}\text{O}_4$

Cations at		I_{220}/I_{440}		I_{400}/I_{422}	
A-site	B-site	Observed	Calculated	Observed	Calculated
$\text{Li}_{0.25}^+, \text{Cu}_{0.5}^{2+}, \text{Fe}_{0.25}^{3+}$	$\text{Fe}_{0.5}^{3+}, \text{Al}_{1.5}^{3+}$		0.303		4.103
$\text{Al}_{0.4}^{3+}, \text{Fe}_{0.6}^{3+}$	$\text{Cu}_{0.5}^{2+}, \text{Li}_{0.25}^+, \text{Fe}_{0.15}^{3+}, \text{Al}_{1.1}^{3+}$		2.439		1.049
$\text{Li}_{0.15}^+, \text{Fe}_{0.35}^{3+}, \text{Al}_{0.5}^{3+}$	$\text{Li}_{0.1}^+, \text{Cu}_{0.5}^{2+}, \text{Fe}_{0.4}^{3+}, \text{Al}_{1.1}^{3+}$	0.514	0.518	1.640	1.641
$\text{Cu}_{0.5}^{2+}, \text{Fe}_{0.5}^{3+}$	$\text{Li}_{0.25}^+, \text{Fe}_{0.25}^{3+}, \text{Al}_{1.5}^{3+}$		0.295		4.375
$\text{Fe}_{0.75}^{3+}, \text{Li}_{0.25}^+$	$\text{Cu}_{0.5}^{2+}, \text{Al}_{1.5}^{3+}$		0.208		4.103
Al^{3+}	$\text{Li}_{0.25}^+, \text{Cu}_{0.5}^{2+}, \text{Fe}_{0.75}^{3+}, \text{Al}_{0.5}^{3+}$		0.494		4.978

TABLE III Comparison of intensity ratios for $\text{Li}_{0.25}\text{Cu}_{0.5}\text{Fe}_{2.25}\text{O}_4$ and $\text{Li}_{0.25}\text{Cu}_{0.5}\text{Al}_{2.25}\text{O}_4$

Cations at		I_{220}/I_{440}		I_{400}/I_{422}	
A-site	B-site	Observed	Calculated	Observed	Calculated
$\text{Li}_{0.25}\text{Cu}_{0.5}\text{Fe}_{2.25}\text{O}_4$					
Fe^{3+}	$\text{Li}_{0.25}^+, \text{Cu}_{0.5}^{2+}, \text{Fe}_{1.25}^{3+}$	0.761	0.760	1.223	1.221
$\text{Li}_{0.25}^+, \text{Fe}_{0.75}^{3+}$	$\text{Cu}_{0.5}^{2+}, \text{Fe}_{0.5}^{3+}$		0.598		1.731
$\text{Cu}_{0.5}^{2+}, \text{Fe}_{0.5}^{3+}$	$\text{Li}_{0.25}^+, \text{Fe}_{1.75}^{3+}$		0.435		1.072
$\text{Li}_{0.25}\text{Cu}_{0.5}\text{Al}_{2.25}\text{O}_4$					
$\text{Li}_{0.25}^+, \text{Al}_{0.75}^{3+}$	$\text{Cu}_{0.5}^{2+}, \text{Al}_{1.5}^{3+}$	0.288	0.287	6.588	6.490
$\text{Cu}_{0.5}^{2+}, \text{Al}_{0.5}^{3+}$	$\text{Li}_{0.25}^+, \text{Al}_{1.75}^{3+}$		0.488		1.106
Al^{3+}	$\text{Li}_{0.25}^+, \text{Cu}_{0.5}^{2+}, \text{Al}_{1.25}^{3+}$		0.189		12.511

also observed that as the value of x increases, Li^+ migrates from the octahedral to the tetrahedral site on replacing Fe^{3+} . The ionic configuration of the system can be written as



3.2. Transport properties

The d.c. resistivity of the system $\text{Li}_{0.25}\text{Cu}_{0.50}\text{Fe}_{2.25-x}\text{Al}_x\text{O}_4$, when measured as a function of temperature, varied between 10^3 and $10^6 \Omega \text{ cm}$. A plot of $\log \rho$ against $10^3/T$ are shown in Fig. 1. All the compositions of the system were semiconductors, and exhibited a linear nature obeying Wilson's law

$$\rho = \rho_0 \exp(-\Delta E/KT) \quad (2)$$

where ρ is resistivity.

The activation energy, ΔE , values for different compositions varied between 0.397 and 0.675 eV (Table I). It is further observed that ΔE increases with an increase in aluminium content, indicating a difficulty in charge transfer in aluminium-rich compounds.

The electrical conductivity, σ , is related to the number of charge carriers, n , and their mobility, μ , at room temperature by the equation

$$\sigma = ne\mu \quad (3)$$

Taking the unit cell volume as $(0.8236 \text{ nm})^3$, the value of the hole concentration comes out to be 10^{22} cm^{-3} . Mobility, μ , values calculated from the above equation are found to be of the order of $10^{-7} \text{ cm}^2 \text{ V}^{-1} \text{ s}^{-1}$. The mobility of charge carriers can also be calculated

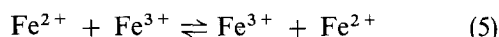
using the equation

$$\mu = \frac{ed^2v \exp(-\Delta E/KT)}{KT} \quad (4)$$

comes out to be $10^{-7} \text{ cm}^2 \text{ V}^{-1} \text{ s}^{-1}$. Low values for oxidic spinels have also been reported by Jain and Darshane [6] and Khan *et al.* [7].

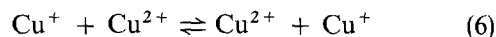
In the case of low-mobility semiconductors, the influence of temperature on the number of charge carriers is very small, and activation energy is associated with mobility of charge carriers rather than with their concentration. The charge carriers can be considered as localized at the ions or the vacant sites, and conduction takes place by hopping of charge carriers between occupied and unoccupied sites. Due to lattice vibrations, the ions occasionally come close enough for the transfer of charge carriers. The conduction is, therefore, induced by lattice vibrations and as a result, the carrier mobility shows an exponential temperature dependence with activation energy.

In the present system, electrical conduction can take place by the hopping of charge carriers (Fe and/or Cu) at the octahedral sites. The electrical conduction in $\text{Li}_{0.25}\text{Cu}_{0.50}\text{Fe}_{2.25}\text{O}_4$ can be explained as follows:



It is quite likely that a small amount of Fe^{2+} must have been formed during heating [8] which could not be detected by X-ray intensity studies. In the last compound of the series, i.e. $\text{Li}_{0.25}\text{Cu}_{0.50}\text{Al}_{2.25}\text{O}_4$, it is observed from intensity data that the copper is present only in the +2 oxidation state; if this had been the

case, then $\text{Li}_{0.25}\text{Cu}_{0.50}\text{Al}_{2.25}\text{O}_4$ would have shown insulating behaviour. However, it is a semiconductor with $\Delta E = 0.675 \text{ eV}$. It is possible that a small amount of Cu^+ must have been formed due to thermal fluctuation which can be represented by the following equation:



This kind of mechanism has been suggested by Kushnerev *et al.* [9] in lithium substituted cobalt manganese.

From Table I, it is observed that activation energy increases ($x = 0$, $\Delta E = 0.397 \text{ eV}$) with increase in concentration of aluminium ions at the octahedral site ($x = 2.25$, $\Delta E = 0.675 \text{ eV}$). Increase in activation energy may be due to exchange of electron transfer.

The plot of thermoelectric power, ΔV , developed across the compounds against temperature difference, ΔT , for all the compositions of the system is shown in Fig. 2. The thermoelectric coefficient, α , determined from the slopes of the plot are given in Table I. The sign of α is designated as positive indicating *p*-type conduction, and negative for *n*-type conduction.

From the compositions investigated, it can be seen that both types of charge carrier are present (Fig. 2). The thermoelectric coefficient, α , in any given case is related to positive and negative charge carriers and conductivity by the equation

$$\alpha = \frac{\alpha_h \sigma_h + \alpha_e \sigma_e}{\sigma_h + \sigma_e} \quad (7)$$

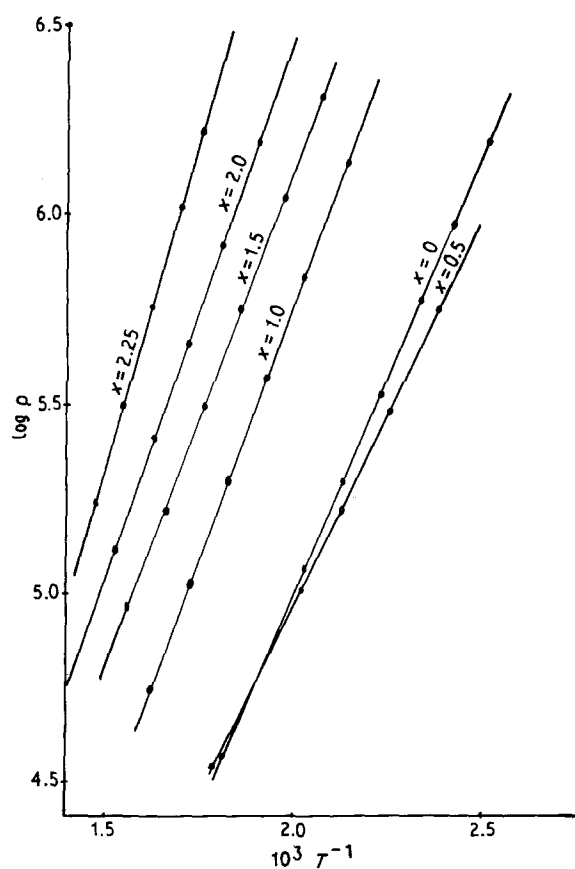


Figure 1 Plot of $\log \rho$ against $10^3 T^{-1}$ for the system $\text{Li}_{0.25}\text{Cu}_{0.5}\text{Fe}_{2.25-x}\text{Al}_x\text{O}_4$.

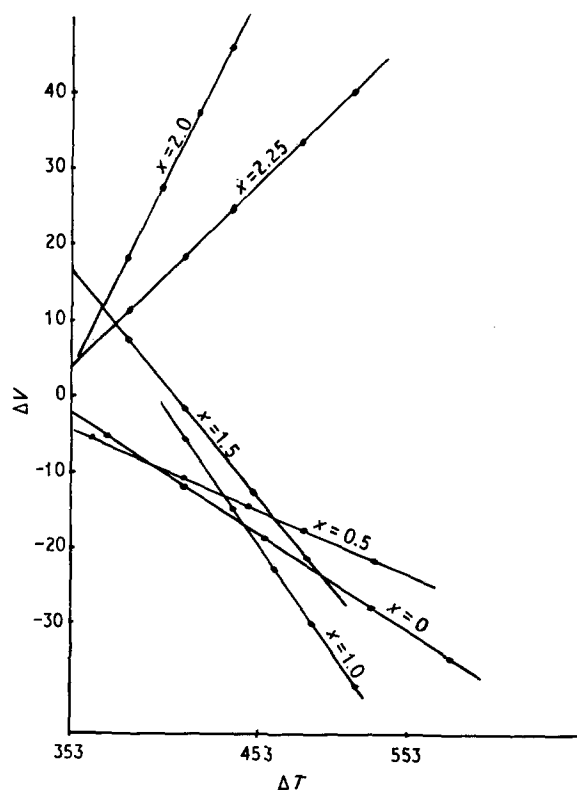


Figure 2 Plot of ΔV against ΔT for the system $\text{Li}_{0.25}\text{Cu}_{0.5}\text{Fe}_{2.25-x}\text{Al}_x\text{O}_4$.

where h and e are p - and n -type charge carriers, respectively. In the present system, it is observed that the compounds $0.0 \leq x \leq 1.5$ are n -type semiconductors and compounds with $2.0 \leq x \leq 2.25$ are p -type semiconductors. Iron-rich compounds are n -type semiconductors, whereas aluminium-rich compounds are p -type semiconductors.

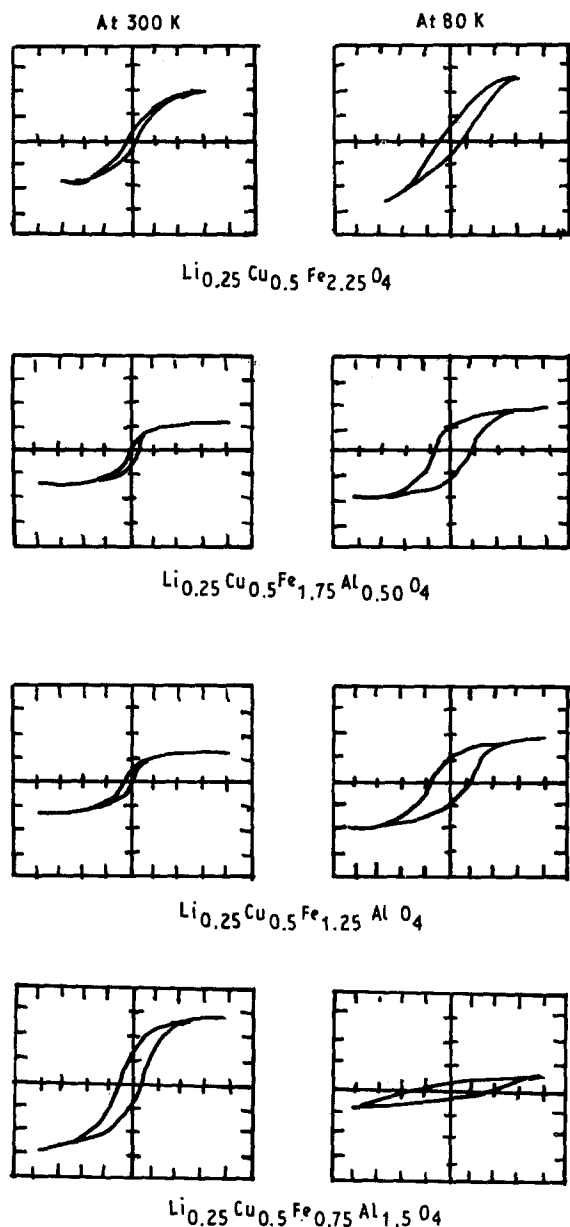


Figure 3 Hysteresis loops for the compounds of the system $\text{Li}_{0.25}\text{Cu}_{0.5}\text{Fe}_{2.25-x}\text{Al}_x\text{O}_4$, ($0 \leq x \leq 1.5$).

3.3. Magnetic hysteresis studies

All the compounds of the system except $x = 2.0$ and $x = 2.25$ show the magnetic hysteresis loops at 300 K as well as at 80 K (Fig. 3). This indicates that they are all ferrimagnetic in nature. The coercive force, H_c , remanance ratio (J_R/J_S), saturation magnetization, σ_s , and magnetic moment, n_B , are listed in Table IV. The magnetic moments were calculated from σ values at 80 K by using the relation

$$n_B = \frac{\sigma_s \times \text{molecular weight}}{5585} \quad (8)$$

The observed n_B values obtained by using the above equation were compared with the calculated n_B values on the basis of spin-only moments (Table IV).

The compounds with $x = 2.0$ and 2.25 do not give any hysteresis loop at an applied field of 3 KOe even at 80 K, indicating that the magnetic ordering temperature is below 80 K and the compounds are not ferrimagnetic. This could be due to strong antiferromagnetic interactions at the B-site, even though A–B interactions exist in these compounds.

It can be seen from Table IV that for $0 \leq x \leq 1.5$, as the concentration of Fe^{3+} decreases and that of Al^{3+} increases, the observed n_B values are lower than the calculated n_B values. The observed low magnetic moments can be explained in terms of the non-collinear spin arrangement. Such behaviour (lower values of n_B than expected) have also been observed by many others in zinc-containing ferrites. This has been explained using various models such as (i) the occupation of B-sites by diamagnetic ions; (ii) the development of paramagnetic clusters; and (iii) the occurrence of non-collinear spin structures, [10, 11]. Pettit and Forester [12] have indicated that the non-collinear magnetic structure plays an important role in the explanation of this behaviour in the oxidic spinel system $\text{Co}_{1-x}\text{Zn}_x\text{Fe}_2\text{O}_4$. The canting in this system has been interpreted in terms of a uniform Yafet–Kittel triangular-type magnetic ordering of spins at the B-sublattice. Thus considering the Yafet–Kittel model [10], we can also explain the variation observed in n_B values for the aluminium-rich compounds of the present system.

From the magnetic hysteresis loops (Fig. 3), it is seen that all the compounds except $x = 2.0$ and $x = 2.25$ possess high values of coercive force, H_c , which may be due to the presence of anisotropy in

TABLE IV Saturation magnetization, σ_s , coercive force, H_c , magnetic moment, n_B , and remanance ratio (J_R/J_S) values for the system $\text{Li}_{0.25}\text{Cu}_{0.5}\text{Fe}_{2.25-x}\text{Al}_x\text{O}_4$

Compound	H_c (Oe)		σ (emug ⁻¹)		n_B (μB)		J_R/J_S	
	300 K	80 K	300 K	80 K	Obs.	Calc.	300 K	80 K
$\text{Li}_{0.25}\text{Cu}_{0.5}\text{Fe}_{2.25}\text{O}_4$	116.7	112.9	59.3	63.56	2.54	5.75	0.32	0.33
$\text{Li}_{0.25}\text{Cu}_{0.5}\text{Fe}_{1.75}\text{Al}_{0.5}\text{O}_4$	101.12	95.34	30.79	34.16	1.28	4.25	0.42	0.40
$\text{Li}_{0.25}\text{Cu}_{0.5}\text{Fe}_{1.25}\text{Al}\text{O}_4$	97.97	144.58	8.72	9.12	1.26	3.95	0.45	0.50
$\text{Li}_{0.25}\text{Cu}_{0.5}\text{Fe}_{0.75}\text{Al}_{1.5}\text{O}_4$	95.45	125.55	7.9	7.9	1.19	1.25	0.50	0.39
$\text{Li}_{0.25}\text{Cu}_{0.5}\text{Fe}_{0.25}\text{Al}_2\text{O}_4$	–	–	–	–	–	–	–	–
$\text{Li}_{0.25}\text{Cu}_{0.5}\text{Al}_{2.25}\text{O}_4$	–	–	–	–	–	–	–	–

these compounds. Further, higher values of H_c observed at 80 K may be due to increase in thermal vibrations. This increase in H_c with decreasing temperature can also be attributed to a rapid increase in the anisotropy constant on cooling [13]. The presence of single-domain grains in these compounds are confirmed by the considerable increase in remanance ratios (J_R/J_S) at 80 K (Table IV) [14].

3.4. Infrared spectra

All the compounds show two bands at about 616 and 480 cm^{-1} (Fig. 4). The band positions for all the compounds are in good agreement with those reported earlier by Preudhomme and Tarte [15] and White and De Angelis [16]. The band positions and threshold frequency are listed in Table V. The threshold frequency for the electronic transition is found to be decreasing with increasing Fe^{3+} concentration. This is in agreement with the trend observed for the activation energy (ΔE) as seen from Table I.

Tarte and Collongues [17] have observed that in normal ferrites, both the absorption bands depend on the nature of octahedral cations and do not significantly depend upon the nature of the tetrahedral ions. However, Waldron [18] and Hafner [19] attributed the band around 600 cm^{-1} to the intrinsic vibrations of tetrahedral complexes, and the band around 400 cm^{-1} to those of octahedral complexes. The difference in band position is because of the difference in the $\text{Fe}^{3+}-\text{O}^{2-}$ distance for octahedral and tetrahedral complexes. It is well known that the vibrational frequencies depend on the cation mass, cation-oxygen bonding force, distance and unit cell parameter.

The presence of Fe^{2+} ions in the ferrites causes a shoulder or splitting of the absorption band [20]. In the case of our investigated compounds, both the bands do not show any shoulder or splitting indicating the absence of Fe^{2+} ions.

4. Conclusion

From the above studies, it can be concluded that the system $\text{Li}_{0.25}\text{Cu}_{0.50}\text{Fe}_{2.25}\text{Al}_x\text{O}_4$ is crystallized out cubic in the range of $0.0 \leq x \leq 2.25$. The compositions where $x = 0.0, 0.50, 1.0$ and 1.50 are n -type, while those $x = 2.0$ and 2.25 are p -type semiconductors. From X-ray intensity, magnetic hysteresis and IR studies it is observed that as the value of x increases, Li^+ migrates from the octahedral to the tetrahedral site replacing Fe^{3+} ions. The magnetic hysteresis studies indicate that the compounds in the range $0 \leq x \leq 1.50$ are ferrimagnetic in nature, nearly obeying Neel's collinear model, while for $x = 2.0$ and 2.25 , the compounds exhibit antiferromagnetism. The IR spectra show the presence of two strong absorption bands around 616 and 480 cm^{-1} . Threshold frequencies decrease with an increase of Fe^{3+} ion concentrations.

References

1. J. B. GOODENOUGH, *Prog. Solid State Chem.* **5** (1971) 145.
2. C. P. POOL JR and H. A. FARACH, *Z. Phys.* **B47** (1982) 55.
3. P. RAJ and S. K. KULSHRESHTHA, *J. Phys. Chem. Solids* **31** (1970) 9.

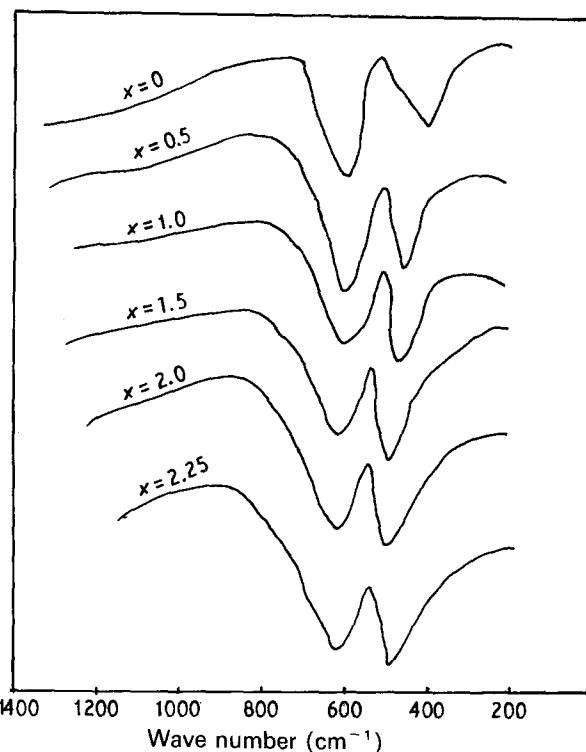


Figure 4 IR spectra of the system $\text{Li}_{0.25}\text{Cu}_{0.5}\text{Fe}_{2.25-x}\text{Al}_x\text{O}_4$.

TABLE V Infrared bands and threshold frequencies for the system $\text{Li}_{0.25}\text{Cu}_{0.5}\text{Fe}_{2.25-x}\text{Al}_x\text{O}_4$

Compound	Absorption bands (cm^{-1})		Threshold frequency (cm^{-1})
	ν_1	ν_2	
$\text{Li}_{0.25}\text{Cu}_{0.5}\text{Fe}_{2.25}\text{O}_4$	600	400	720
$\text{Li}_{0.25}\text{Cu}_{0.5}\text{Fe}_{1.75}\text{Al}_{0.5}\text{O}_4$	616	480	750
$\text{Li}_{0.25}\text{Cu}_{0.5}\text{Fe}_{1.25}\text{Al}_{1.0}\text{O}_4$	616	480	765
$\text{Li}_{0.25}\text{Cu}_{0.5}\text{Fe}_{0.75}\text{Al}_{1.5}\text{O}_4$	605	495	805
$\text{Li}_{0.25}\text{Cu}_{0.5}\text{Fe}_{0.25}\text{Al}_{2.0}\text{O}_4$	610	500	850
$\text{Li}_{0.25}\text{Cu}_{0.5}\text{Al}_{2.25}\text{O}_4$	610	500	910

4. N. P. KAPITONOVA, *Sov. Phys. Solid State* **6** (1965) 2111.
5. A. MILLER, *J. Appl. Phys.* **30** (1959) 245.
6. P. S. JAIN and V. S. DARSHANE, *Nucl. Phys. Solid State Phys. Symp.* **24C** (1981) 529.
7. M. N. KHAN, A. VENKATACHALAM, ASHFAQ AHMED and V. S. DARSHANE, *J. Mater. Sci.* **25** (1990) 595.
8. F. K. LOTGERING, *J. Phys. Chem. Solids* **25** (1964) 95.
9. M. YA. KUSHNEREV, V. R. LINDE and S. Z. ROGIN-SKII, *Sov. Phys. Solid State* **3** (1961) 281.
10. Y. YAFET and C. KITTEL, *Phys. Rev.* **87** (1952) 290.
11. I. NOWICK, *J. Appl. Phys.* **40** (1969) 872.
12. G. A. PETTIT and D. W. FORESTER, *Phys. Rev.* **B4** (1971) 3912.
13. M. TAKAHASHI and M. E. FINE, *J. Appl. Phys.* **43** (1972) 4205.
14. A. E. BERKOTWITZ and W. J. SCHUELE, *ibid.* **30** (suppl.) (1959) 134.
15. J. PREUDHOMME and P. TARTE, *Spectrochim. Acta* **A27** (1971) 961.
16. W. B. WHITE and B. A. DE ANGELIS, *ibid.* **A23** (1967) 985.
17. P. TARTE and R. COLLONGUES, *Ann. Chim (France)* **9** (1964) 135.
18. R. D. WALDRON, *Phys. Rev.* **99** (1955) 1727.
19. S. HAFNER, *Z. Kristallogr.* **115** (1961) 331.
20. V. R. K. MURTHY, S. CHITRA SANKAR, K. V. REDDY and J. SOBHANDARI, *Ind. J. Pure Appl. Phys.* **16** (1978) 79.

Received 4 April
and accepted 30 July 1991